

Introduction

Estimating reservoir property change during a period of production from 4D seismic data has been a concentrated challenge and ambition for geoscientists in the oil and gas industry. These estimates can contribute to a better history matching of the reservoir simulation and for more comprehensive reservoir monitoring.

With the advance of machine learning techniques on all fronts in the geosciences we can address what roles machine learning can take in the established pressure and saturation inversion workflows and what other new workflows can be constructed using this tool. Machine learning is such a broad concept that it can be incorporated at different levels on all the current well established workflows to diminish their weaknesses, bringing more value to the pressure and saturation estimations from seismic inversion. Not only that, with this tool we can create completely new workflows that we are only beginning to grasp.

Here we will present results for two separate methodologies of seismic inversion to changes in pressure and saturation. The first method is a well established model-based Bayesian inversion method using a calibrated petro-elastic model and convolution workflow as the forward seismic modeling operator. In the second method we use a deep neural network to model the inversion process, we use synthetic seismic data to train the network, then apply the inversion to observed data. The methods are applied to the same field data giving a nice platform to compare the neural network inversion results to a more conventional approach.

Schiehallion Data

The inversions are applied to maps of Schiehallion's upper T31 sandstone. It is a fairly thin reservoir (5-30m), which is well defined in the seismic data by one single trough. For this reason, a map-based approach is appropriate. Schiehallion is a highly compartmentalized field with initial pressure close to bubble point pressure. Production in this complex structure led to areas with strong pressurization due to water injection into closed compartments, while other areas lack the pressure support and experience gas release due to pressure depletion. We face the challenge of inverting 4D seismic data to changes in pressure, water saturation and gas saturation (ΔP , ΔS_w and ΔS_g), so the methods need to deal properly with the non-linearities due to each of these effects. The seismic data analysed is a set of eight vintages (from 1996 to 2010). These were reprocessed by CGG in 2014, following a 4D driven multi-vintage workflow. The processing workflow was carefully optimized to maintain 4D AVO amplitudes intact. Synthetic feasibility studies showed that the 4D AVO attributes are in line with the theoretical expectations. The seismic data used for inversion is the 4D difference of the sum of negative amplitudes (ΔSNA) map attribute, extracted from three angle-stacks, along the reservoir time window (see figure 2).

Method 1 - Model-based Bayesian inversion

The Bayesian inversion workflow is explained in detail in Corte et al. (submitted 2019). Essentially the workflow uses a petro-elastic model calibrated to the seismic data by Amini (2018) and a convolutional step to model the seismic data. The ΔSNA attribute is then extracted from the synthetic seismic and compared to the real seismic ΔSNA map. Since this is a map-based inversion, all realizations are sampled in map form and then go through a conversion into the vertical reservoir simulation grid in order to run the forward modelling process. We use a monte carlo sampling algorithm to generate thousands of realizations of the full map and from these extract best estimations and uncertainties. This inversion is constructed in a Bayesian model-based form, with the objective of bringing together information from the history matched reservoir simulation and seismic data. Reservoir simulation results for ΔP , ΔS_w and ΔS_g are incorporated as prior knowledge, to settle ambiguities and lack of seismic information. Where the seismic data lacks information about a certain property the method will bring this information from the simulation model. The inversion results will deviate from the simulation in areas where the seismic data contains enough consistent information to indicate an update is necessary.

Method 2 - Neural network inversion

We use a deep neural network to model the inversion process, based on the synthetic convolution seismic data. Although convolutional neural networks are considered the state of the art in spatially correlated data, we show that a sample-wise feed forward neural network trained on noise-free convolutional seismic can invert observed seismic data. We aim to build a regression model that can invert physical seismic angle stack data to pressure and saturation data.

Distinguishing pressure and saturation changes in 4D seismic data is a hard to solve problem. In neural networks, this is no different. The variation of data showing different pressure and saturation change scenarios is sparse, which complicates training and may possibly be disregarded as noise. This increases the need for training data immensely. However, we can include prior physical insights into neural networks to reduce the cost of training and uncertainty. As neural networks are at its basis very large mathematical functions, we can explicitly calculate the P-wave AVO gradient within the network to use as additional information source, without the need of feeding it into the network as input data. This has the added benefit of the network learning on noisy gradients. The design choice for the neural networks can be arbitrary, however, encoder-decoder networks have proven to force neural networks to find meaningful relationships within the data and reduce to these in the bottleneck or embedding layer. For the final architecture we used *hyperopt* (Bergstra et al., 2013) and *keras* (Chollet, 2015). This allows us to use a Tree of Parzen (TPE) estimator for hyperparameter estimation. The estimator models $P(x|y)$ and $P(y)$, where y the quality of fit and x is the hyperparameter set drawn from a non-parametric density (Bergstra et al., 2011).

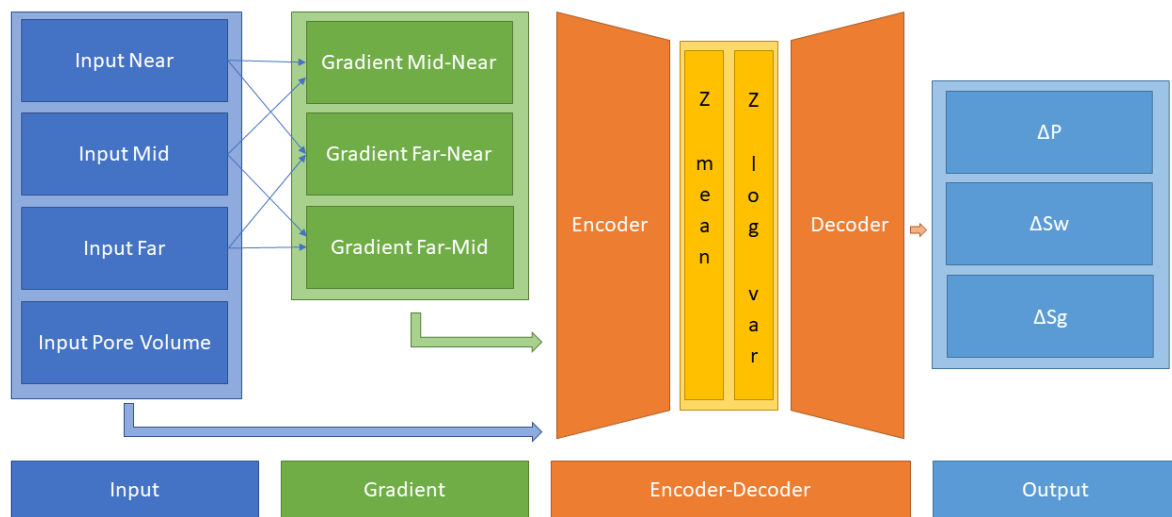


Figure 1 Architecture for sample-based seismic inversion with explicit gradient calculation.

The architecture is shown in figure 1. Inputs are Near, Mid, Far seismic, and Pore volume. These Input Layers are passed on to calculate the mid-near, far-mid, and far-near gradients. These four inputs and three gradients are concatenated and fed to the encoder. z_mean and z_log_var build the variational embedding with z_Lambda being the sampler fed to the decoder network. The decoder splits into three output layers ΔP , ΔSw , and ΔSg .

The network is trained using *sim2seis* results calculated for the seven time-steps at seismic monitor acquisition times, it is then used to invert each seismic monitor individually. The inversion results for the synthetic data gave a consistent R^2 -score of over 0.6 for all simultaneous inversion targets ΔP , ΔSw and ΔSg with an encoder-decoder architecture and a deterministic embedding layer. While we kept the main architecture constant, we replaced the embedding layer with a variational formulation to allow for noise in the input to output mapping added noise injection to the input layer, to apply Gaussian Noise during the training phase. This significantly improved the inference on observed seismic data. The total training time for the network was 3 hours on a K5200 GPU, prediction speed takes $5.11 s \pm 22.1 ms$.

Schiehallion Field Data Example

The field data differs significantly from the synthetic data in that it is noisier, assuming the same ground truth. This is a true challenge for a sample-wise process to produce consistent results. We have trained the network with Gaussian noise on the input data with zero mean and a standard deviation of $\sigma = .02$, therefore, approximately 95 % of the noise may distort up to a maximum 40 % of the clean signal.

Figure 2 shows the observed 4D seismic maps (ΔSNA) for the 2004 monitor acquisition using the 1996 acquisition as baseline. Figure 3 shows, in the first row, the simulation model results (used in the Bayesian method as prior information), in the second row, the inversion results for the Bayesian method, and in the third row, the inversion results for the neural network method.

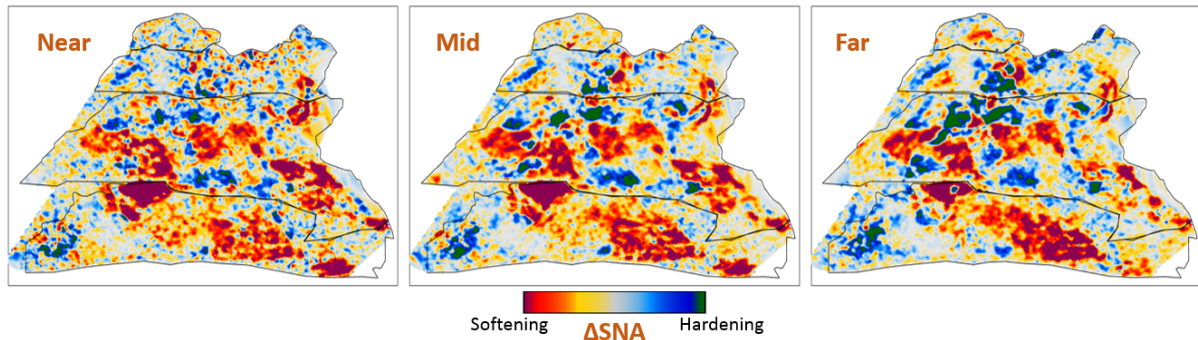


Figure 2 Schiehallion 2004 Timestep Seismic data, pore volume and sim2seis results.

From figure 3 we can see clearly the influence of the prior simulation model in the Bayesian results. The neural network does not use a prior, so the results are not influenced by the simulation model and can be seen as a direct interpretation of the seismic data. Comparing both we can see what bits of information the Bayesian method is bringing from the prior. The seismic data is most sensitive to gas saturation changes, so the Bayesian method is able to capture this consistent information from seismic data and deviate ΔSg results from the initial prior. The results for gas saturation are the most in agreement in both methods precisely because all this information is coming from the seismic data. We see some leakage of hardening effects into the ΔSg results in method 2 due to the fact that we cannot set constraints to that inversion process. Since there is no initial gas saturation in those areas the saturation change cannot be negative, these comprehensive constraints are imbedded into the Bayesian workflow but not in the neural network.

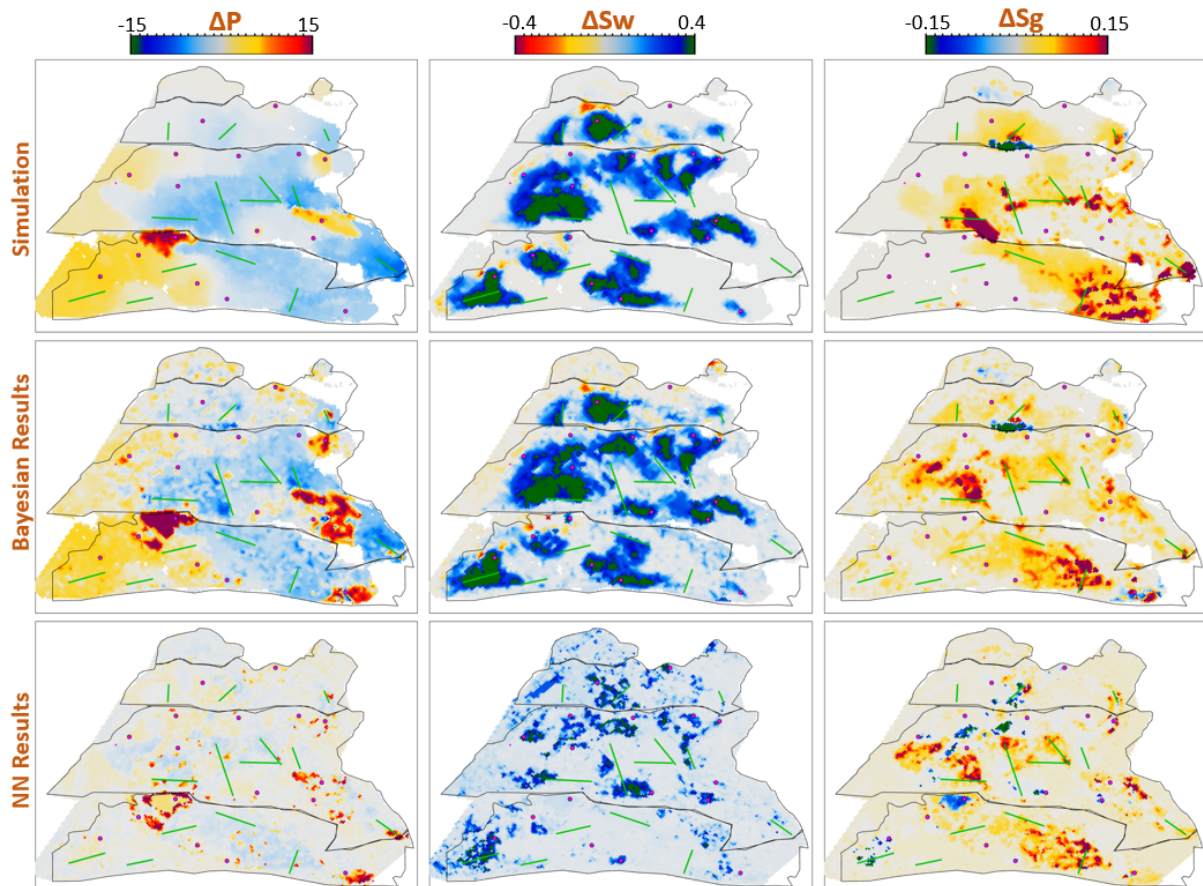


Figure 3 Schiehallion 2004 Timestep Bayesian Inversion and Neural Inversion

Water saturation has a distinctive hardening effect on seismic data, but in this map it is highly obscured by stronger overlying softening effects due to pressure increase and gas breakout. The neural network interprets all the hardening anomalies correctly as water saturation increase, while controlling for noise in areas of softening amplitudes. In those areas the seismic data does not contain useful information on the water saturation so the Bayesian result relies on a strong prior to compensate. All of the water saturation inverted by method 2 is in agreement with method 1, but since method 1 has this additional information from the prior, the map seems more coherent.

The pressure effect on seismic is highly non-linear. While high increases in pressure show a very strong softening effect, milder pressure variations (up to ± 7 MPa) have very little influence on the seismic data and are easily obscured by overlying effects. For this reason, the neural network pressure inversion in regions of mild change is low and often correlated with saturation. The Bayesian inversion benefits from the prior to fill those pressure values. This method does deviate from the prior in areas of strong softening signals due to pressure increase, and those areas are also correctly interpreted by the neural network inversion.

When we relax the prior of the Bayesian inversion, these results are very noisy in the pressure and water saturation estimates. In these areas the neural network inversion is robust to noise. During the neural network training the pore volume has shown to be important in guiding the inversion from the seismic data. Adding pore volume data adds a structural component to the neural inversion process, which improves the overall results from the sample-based method significantly.

Conclusions

This work presents Deep Neural Inversion of 4D seismic data. We compare the results with a Bayesian Inversion approach. We show that Deep Neural Networks can model seismic inversion trained on synthetic data. Explicit calculation of the P-wave AVO gradient within the network stabilizes the pressure-saturation separation within the network and Noise Injection enables the transfer to unseen seismic field data. Neural networks can be an important tool to investigate nascent information in 4D seismic data to improve inversion workflows and reduce uncertainty in seismic analysis.

The Neural Inversion can be used as a valuable tool to explore purely data-based inversion results in the presence of noise. It is able to translate the ambiguous seismic amplitudes into much more easily interpreted property maps. The value of the Bayesian inversion results presented is in combining all knowledge about the reservoir to create a general view of the reservoir dynamics. These results show the current understanding of reservoir dynamics updated by imprinting seismic information on top of the history matched simulation results.

Acknowledgements

The research leading to these results has received funding from the Danish Hydrocarbon Research and Technology Centre under the Advanced Water Flooding program. We thank the sponsors of the Edinburgh Time-Lapse Project, Phase VII (AkerBP, BP, CGG, Chevron, ConocoPhillips, ENI, Equinor, ExxonMobil, Halliburton, Nexen, Norsar, OMV, Petrobras, Shell, Taqa, and Woodside) for supporting this research. The Brazilian governmental research-funding agency CNPq. We are also grateful to Linda Hodgson and Ross Walder for important discussions on the field and dataset. We thank Mikael L  thje for valuable feedback.

References

- Amini, H. [2018] Comparison of Xu-White, Simplified Xu-White (Keys & Xu) and Nur's Critical Porosity in Shaley Sands. In: *80th EAGE Conference and Exhibition 2018*.
- Bergstra, J., Yamins, D. and Cox, D.D. [2013] Making a science of model search: Hyperparameter optimization in hundreds of dimensions for vision architectures.
- Bergstra, J.S., Bardenet, R., Bengio, Y. and K  gl, B. [2011] Algorithms for Hyper-Parameter Optimization. In: Shawe-Taylor, J., Zemel, R.S., Bartlett, P.L., Pereira, F. and Weinberger, K.Q. (Eds.) *Advances in Neural Information Processing Systems 24*, Curran Associates, Inc., 2546–2554.
- Chollet, F. [2015] Keras. <https://github.com/fchollet/keras>.
- Corte, G., MacBeth, C. and Amini, H. [submitted 2019] North Sea field application of 4D Bayesian in-

version to pressure and saturation changes. In: *81st EAGE Conference & Exhibition 2019*. Submitted.